Microbial methanogenesis in the sulfate-reducing zone of surface sediments traversing the Peruvian margin

Johanna Maltby[a*], Stefan Sommer[a], Andrew W. Dale[a], Tina Treude[a,b*]

[a] *GEOMAR Helmholtz Centre for Ocean Research Kiel, Department of Marine Biogeochemistry, Wischhofstr. 1-3, 24148 Kiel, Germany*

[b] *Present address: Department of Earth, Planetary & Space Sciences and Atmospheric & Oceanic Sciences, University of California, Los Angeles (UCLA), CA, USA*

Correspondence: jmaltby@geomar.de, ttreude@g.ucla.edu

Abstract

We studied the concurrence of methanogenesis and sulfate reduction in surface sediments (0-25 cm below seafloor) at six stations (70, 145, 253, 407, 990 and 1024 m) along the Peruvian margin (12°S). This oceanographic region is characterized by high carbon export to the seafloor creating an extensive oxygen minimum zone (OMZ) on the shelf, both factors that could favor surface methanogenesis. Sediments sampled along the depth transect traversed areas of anoxic and oxic conditions in the bottom-near water. Net methane production (batch incubations) and sulfate reduction (^{35}S-sulfate radiotracer incubation) were determined in the upper 0-25 cmbsf of multiple cores from all stations, while deep hydrogenotrophic methanogenesis (> 30 cmbsf, ^{14}C-bicarbonate radiotracer incubation) was determined in two gravity cores at selected sites (78 and 407 m). Furthermore, stimulation (methanol addition) and inhibition (molybdate addition) experiments were carried out to investigate the relationship between sulfate reduction and methanogenesis.

Highest rates of methanogenesis and sulfate reduction in the surface sediments, integrated over 0-25 cmbsf, were observed on the shelf (70-253 m, 0.06-0.1 mmol m^{-2} d^{-1} and 0.5-4.7 mmol m^{-2} d^{-1}, respectively), while lowest rates were discovered at the deepest site (1024 m, 0.03 and 0.2 mmol m^{-2} d^{-1}, respectively). The addition of methanol resulted in significantly higher surface methanogenesis activity, suggesting that the process was mostly based on non-competitive substrates, i.e., substrates not used by sulfate reducers. In the deeper sediment horizons, where competition was probably

relieved due to the decrease of sulfate, the usage of competitive substrates was confirmed by the detection of hydrogenotrophic activity in the sulfate-depleted zone at the shallow shelf station (70 m). Surface methanogenesis appeared to be correlated to the availability of labile organic matter (C/N ratio) and organic carbon degradation (DIC production), both of which support the supply of methanogenic substrates. A negative correlation between methanogenesis rates and dissolved oxygen in the bottom-near water was not obvious, however, anoxic conditions within the OMZ might be advantageous for methanogenic organisms at the sediment-water interface.

Our results revealed a high relevance of surface methanogenesis on the shelf, where the ratio between surface to deep (below sulfate penetration) methanogenic activity ranged between 0.13 and 10^5. In addition, methane concentration profiles indicated a partial release of surface methane into the water column as well as consumption of methane by anaerobic methane oxidation (AOM) in the surface sediment. The present study suggests that surface methanogenesis might play a greater role in benthic methane budgeting than previously thought, especially for fueling AOM above the sulfate-methane transition zone.

Keywords: Oxygen minimum zone, organic matter, competition, anaerobic oxidation of methane, emission

1. Introduction

Microbial methanogenesis represents the terminal step of organic matter degradation in marine sediments (Jørgensen, 2006). The process is entirely restricted to a small group of prokaryotes within the domain of the Archaea (Thauer, 1998). Methanogens produce methane from a narrow spectrum of substrates, primarily carbon dioxide (CO_2) and hydrogen (H_2) (hydrogenotrophic pathway), as well as acetate (acetoclastic pathway) (Zinder, 1993). In addition, methanol or methylated compounds such as methylamine can be utilized (methylotrophic pathway) (Oremland & Polcin, 1982; Buckley et al., 2008; Zinder, 1993; King et al., 1983). Substrates for methanogenesis are produced during depolymerization and fermentation of organic macromolecules (e.g., sugars, vitamins, amino acids) to

smaller monomeric products (Jørgensen, 2006; Schink & Zeikus, 1982; Neill et al., 1978; Donnelly & Dagley, 1980).

Acetoclastic and hydrogenotrophic methanogenesis are predominantly found in deeper sediment zones below sulfate penetration, owing to the more effective utilization of H_2 and acetate by sulfate reducers due to their higher substrate affinity (Oremland & Polcin 1982; Jørgensen 2006).Methanogens can avoid competition with sulfate reducers by the utilization of non-competitive substrates, such as methanol or methylamines (Oremland & Polcin, 1982; King et al., 1983). Facilitated by the usage of such non-competitive substrates, sulfate reduction and methanogenesis were found to co-occur in sulfate-containing salt marsh sediments (Oremland et al., 1982; Buckley et al., 2008; Senior et al., 1982). Concurrent activity of sulfate reduction and methanogenesis in the marine environment has mostly been postulated for organic-rich sediments (Mitterer, 2010; Jørgensen & Parkes, 2010; Treude et al., 2009, 2005a; Hines & Buck, 1982; Crill & Martens, 1986); however, details on the magnitude and environmental controls of surface methanogenesis are still poorly understood (Holmer & Kristensen, 1994; Ferdelman et al., 1997).

In a study from Eckernförde Bay, southwestern Baltic Sea, considerable in vitro methanogenic activity was observed in samples taken from 5 to 40 cm sediment depth (Treude et al. 2005). Although in vitro activity was measured in sulfate-free setups, methanogenic activity coincided with zones of in-situ sulfate reduction. The authors concluded a coexistence of the two types of organisms, which could be enabled through either the usage of non-competitive substrates, dormancy of methanogens until phases of sulfate depletion, and/or temporal or spatial heterogeneity in the sediments. Eckernförde Bay sediments feature a high input of organic matter due to a shallow water depth (~30 m) and pronounced phytoplankton blooms in spring, summer, and fall (Smetacek, 1985). Furthermore, seasonal hypoxia (O_2 < 90 µM) or even anoxia (O_2=0 µM) occur in the deep layers of the water column caused by stratification and degradation of organic matter (Bange et al. 2011). Oxygen-depleted conditions in the bottom water together with frequent input of fresh organic matter possibly favors methanogenesis in surface sediment by offering reduced conditions and non-competitive substrates. As non-competitive substrates can be derived from organic osmolytes such as betaine or dimethylsulfoniopropionate (DMSP), a high load of organic matter (e.g. through sedimentation of

84 phytoplankton blooms) can increase the availability of non-competitive substrates (Zinder, 1993; Van
85 Der Maarel & Hansen, 1997). In accordance, methanogenesis activity was observed within the sulfate-
86 reducing zone of organic-rich sediments from the seasonally hypoxic Limfjorden sound, Northern
87 Denmark (Jørgensen & Parkes, 2010; Jørgensen, 1977).
88
89 The environmental relevance of surface methanogenesis is hitherto unknown. Its closeness to the
90 sediment-water interface makes it a potential source for methane emissions into the water column,
91 unless the methane is microbially consumed before escaping the sediment (Knittel & Boetius, 2009).
92 Methane escapes the sediment either by diffusion or, when methane saturation is exceeded, in the form
93 of gas bubbles (Whiticar, 1978; Wever & Fiedler, 1995; Judd et al., 1997; Dimitrov, 2002). The
94 fraction of methane released to the water column that reaches the atmosphere mainly depends on
95 water depth, as methane is also consumed within the water column through aerobic microbial
96 oxidation (Reeburgh, 2007; Valentine et al., 2001). Thus, shallow coastal areas have higher methane
97 emission potentials than the open ocean (Bange et al., 1994) and a greater potential to contribute to
98 methane-dependent atmospheric warming (IPCC, 2014).
99
100 In the present study we focused on the upwelling region off the Peruvian coast, which is another
101 example of an environment where both factors that potentially favor surface methanogenesis convene,
102 i.e., a high export of organic carbon and low dissolved oxygen concentrations in the bottom water.
103 This upwelling region represents one of the most productive systems in the world oceans, creating one
104 of the most intense oxygen minimum zones (OMZ, Kamykowski & Zentara 1990; Pennington et al.
105 2006). Oxygen concentrations in waters impinging on the seafloor are below 20 µM or even reach
106 anoxia. Research on surface sediment methanogenesis in upwelling regions is scarce and its potential
107 role in the carbon cycling of the Peruvian OMZ is completely unknown. In a study from the central
108 Chilean upwelling area (87 m water depth, 0.5-6 cm sediment depth), low methane production rates
109 were detected despite high sulfate reduction activity, when the non-competitive substrate
110 trimethylamine was offered (Ferdelman et al., 1997). The authors concluded that the prevailing

methanogens were competing with sulfate reducers for H_2 and with acetogens for methylamines, explaining the overall low methanogenesis activity observed (Ferdelman et al., 1997).

Even though the Chilean and Peruvian OMZs are connected, commonly known as OMZ in the Eastern South Pacific Ocean (ESP) (Fuenzalida et al., 2009), the core of the ESP-OMZ is centered off Peru with an upper boundary at < 100 m and a vertical distribution to > 600 m versus a thinner OMZ band off Chile constrained between 100-400 m water depth (Fuenzalida et al., 2009). Anoxic conditions in the water column of the OMZ core (and therewith a lack of bioirrigating macrofauna introducing oxygen into the sediments (Kristensen, 2000)) together with the high export rates of labile organic carbon to the seafloor (Reimers & Suess, 1983; Dale et al., 2015) provide favorable conditions for methanogenesis activity in surface sediments, thus increasing the potential for benthic methane emissions.

Here, we provide first insights into surface methanogenesis in sediment cores (< 30 cmbsf = centimeters below seafloor) taken along the Peruvian shelf and margin. We hypothesize that methanogenesis coexists with sulfate reduction through the utilization of non-competitive substrates. In addition, we postulate that surface methanogenesis depends on the quantity and quality (= freshness) of organic carbon, and the concentrations of dissolved oxygen in the bottom water. We therefore expect spatial variability of surface methanogenesis along the continental shelf and margin. The observed methanogenic activity will be compared to methane concentrations in the bottom-near water to discuss the potential relevance of surface methanogenesis for methane emissions into the pelagic zone.

2. Material and Methods

2.1 Study site and sediment sampling

Samples were taken during the R.V. Meteor cruise M92 between 5. Jan and 3. Feb 2013 along a depth transect off the Peruvian coast from the shelf (~70 m) to the continental margin (~1000 m). The transect was located in the central part of the ESP-OMZ (Fuenzalida et al., 2009) at 12°S. Further hydrographic details on the study area can be found elsewhere (Dale et al., 2015).

Sediment cores for the determination of near-surface methanogenesis were collected at six stations along the depth transect at 70, 145, 253, 407, 776 and 1024 m water depth (Fig.1), using a multiple corer with a mounted camera (TV-MUC). The MUC held seven cores (length: 60 cm, inner diameter: 10 cm) and covered an area of ~1 m^2. If necessary, a second MUC was deployed at the same station, thus sediment cores could originate from different MUC casts. Station numbers were assigned in accordance with Dale et al., (2015). After retrieval, sediment cores were transferred to a ~ 9°C cold room and processed at the same day.

In addition to the MUC, a gravity corer was deployed at two stations (78 and 407 m) for determining deep methanogenesis. The total core length was 400 cm and 206 cm, respectively. The gravity corer was equipped with a 260 kg weight and a 5 m steel barrel (diameter: 14 cm). The replaceable core liner (PVC, diameter: 12.5 cm) was housed within the barrel and fixed with a core catcher. After retrieval, sediment cores from the gravity corer were sliced into 1–m sections, capped on both sides, and brought to the cold room (4°C) for further processing. Relevant station details for MUC and gravity cores are summarized in Table 1.

2.2 Water column sampling

CTD/Rosette water column casts were conducted at the same station as sediment coring (for details see Table 1). Temperature and oxygen data were taken from Dale et al. 2015.

For the analysis of methane concentrations in the bottom-near water, water was sampled ca. 1.5 m above the seafloor from 10 L Niskin bottles mounted on the CTD/Rosette r. The collected water was filled bubble-free into 60 ml vials (triplicates), each vial containing 3 pellets of sodium hydroxide (NaOH ,~ 0.3 M per vial) to stop microbial activity and force dissolved gas into the headspace. After closing the vials with a butyl rubber stopper and a crimp seal, 10 ml of water was removed with a N_2-flushed 10 ml syringe and replaced with N_2 gas from a second syringe to create a headspace in the sampling vials. Samples were stored and transported at room temperature until further processing.

In the home laboratory, 100 µl of the headspace volume was injected into a Shimadzu GC-2014 gas chromatograph equipped with a flame ionization detector and a HaySep-T 100/120 column (Length 3 m, diameter: 2 mm). Gases were separated isothermally at 75°C with helium carrier gas. Methane

concentrations were calibrated against methane standards (Scotty gases). The detection limit was 0.1 ppm with a precision of 2 %.

2.3 Porewater geochemistry

Porewater sampling for MUC cores has been previously described by Dale et al., (2015). In short, one MUC core per station was subsampled in an argon-filled glove bag to preserve redox sensitive constituents.

The gravity cores at St. 1 (78 m) and St. 8 (407 m) were subsampled at 10-12 different sediment depths (depending on core length) resulting in depth intervals of 20-33 cm. Before sampling, the plastic core liner was cut open with an electric saw at the specific depths. Porewater was extracted by using anoxic (flushed with argon), wetted rhizons (Rhizosphere Research Products, Seeberg-Elverfeldt et al., 2005).

Sulfate concentrations were determined by ion chromatography (Methrom 761) as described previously by Dale et al., (2015).

For DIC analysis, 1.8 ml of porewater was transferred into a 2 ml glass vial, fixed with 10 µl saturated mercury chloride solution and crimp sealed. Samples were stored at 4°C until further processing in the home laboratory. DIC concentration was determined as CO_2 with a multi N/C 2100 analyzer (Analytik Jena) following the manufacturer's instructions. Therefore the sample was acidified with phosphoric acid and the outgassing CO_2 was measured. The detection limit was 20 µM with a precision of 2-3%.

2.4 Sediment porosity and particulate organic carbon/nitrogen

Methodology and data for porosity, particulate organic carbon (POC) and particulate organic nitrogen (PON) have been previously described by Dale et al., (2015).

In short, wet sediment samples were taken from the porewater MUC core and the gravity cores for determination of porosity from the weight difference of wet and freeze-dried sediment. POC and PON were analyzed with a Carlo-Erba element analyzer (NA 1500). Ratios of POC:PON were calculated by division.

2.5 Sediment methane

For sediment methane concentration, one MUC core per station was sliced in 2 cm intervals until 20 cm depth, followed by 5 cm intervals until the end of the core (maximum depth = 48 cm). Gravity cores were subsampled according to the above scheme (see 2.3). From each sampled sediment layer, 2 cm^{-3} sediment were transferred into a 15 ml serum glass vial containing 5 ml of NaOH (2.5% w/w). The vial was closed with a butyl stopper, crimp sealed and shaken thoroughly to stop microbial activity and to force all methane into the headspace. Vials were stored upside down at room temperature until measurement in the home laboratory.

Sediment methane concentration was determined by injecting 0.1 ml of headspace volume into a Shimadzu GC-2014 gas chromatograph as described under section 2.2.

2.6 Net methanogenesis activity in MUC cores

Sediment from MUC cores was used to determine net methanogenesis, which is defined as the sum of total methane production and consumption, including all available methanogenic substrates in the sediment. Net methanogenesis was determined by measuring the linear increase of methane concentration in the headspace of closed incubation vials over time. Therefore, one MUC core per station was sliced into 5 cm intervals, transferring 10 cm^{-3} of sediment in triplicates into N_2-flushed 60 ml serum glass vials. The sediment core lengths ranged from 25 up to48 cm, resulting in maximum 10 depth intervals. Ten ml of anoxic deep water overlying each MUC core was added to the vial and the slurry was mixed under a constant N_2 stream (Hungate, 1950) before being sealed with a butyl rubber stopper and crimped. The sediment slurry was repeatedly flushed with N_2 through the stopper to ensure fully anoxic conditions. The vials were incubated in the dark and at 9°C, which reflected the average in situ temperature along the depth transect (see Table 1). The first gas chromatographic measurement was done directly after preparation of the vials, by injecting 100 µl of headspace sample into the gas chromatograph. The on-board Hewlett Packard-5890 gas chromatograph was equipped with a flame ionization detector and a HaySep-T 100/120 column (Length 3m, diameter: 2mm). Gases were separated isothermally at 75°C with helium carrier gas. Methane concentrations were calibrated

against methane standards. The detection limit was 1 ppm with a precision of < 5%. Measurements were done in 2-4 day-intervals over a total incubation time of ~2 weeks.

2.7 Potential non-competitive and competitive methanogenesis in sediment slurries from MUC cores

Sediment slurry experiments were conducted with sediment from St. 1 (70 m) to examine the interaction between sulfate reduction and methanogenesis, as this station revealed highest microbial activity of sulfate reduction and methanogenesis. On board, the sediment core was sliced in 5 cm intervals. Sediment from the 0-5 cm interval and the 20-25 cm interval was transferred into 250 ml glass bottles, which were then closed without headspace (filled to top) with a butyl rubber stopper and screw cap. Until further treatment, sediment was stored at 4°C on board and later in a 1°C cold room on shore.

Approximately 6 months after the cruise, sediment slurries from both depth intervals were prepared by mixing 5 ml sediment in a 1:1 ratio with artificial, fully marine seawater (Widdel & Bak, 1992) before further manipulations.

In total, three different treatments, each in triplicates, were prepared per depth: 1) sulfate-rich (28 mM), serving as a control 2) sulfate-rich plus molybdate (22 mM) from now on referred to as molybdate-treatment, and 3) sulfate-rich plus methanol (10 mM) from now on referred to as methanol-treatment.

Molybdate was used as an enzymatic inhibitor for sulfate reduction (Oremland & Capone, 1988). Methanol is a known non-competitive substrate used by methanogens, but not by sulfate reducers (Oremland & Polcin, 1982), which makes it suitable to examine non-competitive methanogenesis.

The sediment slurries were incubated at 9°C in the dark for 23 days and headspace concentration of methane was measured repeatedly over time on a gas chromatograph. Therefore, 100 µl of headspace was removed from the gas vials and injected into a Shimadzu gas chromatograph (GC-2014) equipped with a methanizer (inactive), a packed Haysep-D column and a flame ionization detector. The column temperature was 80°C and the helium flow was set to 12 ml min^{-1}. Methane concentrations were measured against methane standards. The detection limit was 0.1 ppm with a precision of <5%. Rates

were determined from the linear increase of methane concentration over time. Due to differences in the linear increase between the three treatments, rates were determined at two different time points: the first period of incubation includes the starting point (day 0) until day 5, the second period includes day 8 to day 23 (Supplement information, Fig. S1).

Student's t-test (independent, two-tailed, $\alpha = 0.05$) was applied to detect significant differences between the three different treatments.

2.8 Gross hydrogenotrophic methanogenesis activity in gravity cores

For the determination of surface to deep methanogenesis activity in gravity cores the radiotracer technique using ^{14}C-bicarbonate was applied (Jørgensen, 1978). With this method only hydrogenotrophic methanogenesis from CO_2/H_2 can be determined, which is the expected main pathway in deeper sediment layers.

Sampled sediment depths were according to the sampling scheme described under section 2.3. Circa 5 cm^{-3} of sediment was sampled in triplicates into glass tubes equipped with syringe plungers and then sealed headspace-free with butyl rubber stoppers. Then, ^{14}C-bicarbnoate-tracer (dissolved in water, pH = 8-9, injection volume 6 µl, activity 222 kBq, specific activity 1.85-2.22 GBq/mmol) was injected through the stopper. The vials were incubated for 48 hours at 9°C before the reaction was stopped by transferring the sediment into 50 ml glass vials filled with 20 ml NaOH (2.5%), closed with butyl rubber stoppers and shaken thoroughly. Five controls were produced from various sediment depths by injecting the radiotracer directly into the NaOH with sediment.

In the home laboratory, ^{14}C- methane production was determined with the slightly modified method by Treude et al., (2005a) used for the determination of anaerobic oxidation of methane. The method was identical, except that no unlabeled methane was determined by gas chromatography. Instead, DIC values were used to calculate hydrogenotrophic methane production (= CO_2 reduction):

$$MG\ rate = \frac{^{14}CH_4 * [DIC]}{(^{14}CH_4 + ^{14}C\text{-}DIC) * t}$$

The methanogenesis rate (*MG rate*) is expressed in nmol CH_4 cm^{-3} sediment d^{-1}, $^{14}CH_4$ is the activity of produced $^{14}CH_4$, ^{14}C-DIC is the activity of residual radioactive dissolved organic carbon (DIC= CO_2 + HCO_3^- + CO_3^{2-}), [DIC] is the concentration of dissolved organic carbon in nmol cm^{-3} sediment, and t is the incubation time in days.

2.9 Sulfate reduction in MUC cores

One MUC core per station was used for the determination of sulfate reduction. First, two replicate push cores (length 30 cm, inner diameter 2.6 cm) were subsampled from one MUC core. The actual core length varied from 23-25 cmbsf total length. Then, 6 µl (~150 kBq) of carrier-free $^{35}SO_4^{2-}$ radiotracer (dissolved in water, specific activity 37 TBq $mmol^{-1}$) was injected into the replicate pushcores in 1 cm intervals according to the whole-core injection method of Jørgensen, (1978). Push cores were incubated for ca. 12 h at 9°C. After incubation, bacterial activity was stopped by slicing the push core into 1-cm intervals and transferring each sediment layer into 50 ml plastic centrifuge tubes filled with 20 ml zinc acetate (20% w/w). Controls were done in triplicates from different depths. Here, the sediment was first fixed with zinc acetate before adding the tracer. Rates for sulfate reduction were determined using the cold chromium distillation procedure according to Kallmeyer et al., (2004).

The yielded sulfate reduction rates have to be treated with caution, due to long (up to 3 half-life times of ^{35}S) and unfrozen storage. Storage of sulfate reduction samples without freezing has recently been shown to result in the re-oxidation of ^{35}S-sulfides, which results in an underestimation of sulfate reduction rates (Røy et al., 2014). During this reaction, zinc sulfide ($Zn^{35}S$) and iron sulfide ($Fe^{35}S$) are re-oxidized to sulfate by reactive Fe(III), which originates from the reaction of Fe^{2+} with oxygen. Fe^{2+} is released during the gradual conversion of FeS to ZnS, which has the lower solubility product. Still, we do trust the relative distribution of activity along depth profiles and consider a potential underestimation of absolute rates.

3. Results

3.1 Water column oxygen and methane concentration

Dissolved oxygen in the bottom water was below detection limit from St.1 (70 m) to St. 8 (407 m), subsequently increasing with water depth to 53 µM at the deepest site (see Table 1and Dale et al., 2015). At the shallowest St. 1 (70 m) the water was turbid and smelled of sulfide.

Dissolved methane concentrations in the bottom water were high on the shelf (St.1-6, 70-253 m) and 10 fold lower at the deeper sites (St. 8-10, 407-1024 m; Table 1). The highest measured methane concentration was detected at St. 6 (253 m, ~80 nM) and lowest concentrations were detected at St. 10 (1024 m, ~4 nM).

3.2 Sediment core description

A detailed sediment description for the porewater geochemistry cores has been already published in detail by Dale et al., (2015). In short, sediments revealed a grey color with a black surface layer at St. 1 (70 m), a dark olive green color at St. 4-8 (145-407 m), and a green-brown color at St. 9 and 10 (770 -1024 m). Sediment texture was soft and fluffy at St. 1-6 (70-253 m), and was less soft at the deeper sites. St. 8 (407 m) revealed a fluffy surface layer followed by a dense clay layer > 2 cmbsf sediment depth. In addition, phosphorite nodules were found at the sediment surface (0-2 cmbsf) of St. 8 (407 m).

Mats of the sulfur oxidizing bacteria *Thioploca spp*. (Gallardo, 1977) were visible at the sediment surface at St.1-6 (70-253 m), with the densest mat at St. 1 (70 m) continuously decreasing with increasing water depth. Sheaths of *Thioploca* were visible until 20-30 cmbsf at St. 1, 4 and 6 (70-253 m).

Foraminifera could be observed at the sediment surface of St. 8 (407 m), St. 9 (770 m) and St. 10 (1024 m). St. 8 (407 m) showed a thick layer of foraminifera ooze on the sediment surface (0-3 cmbsf) while St. 9 (770 m) and St. 10 (1024 m) showed only scattered foraminifera at the sediment surface (0-5 cmbsf).

328 Macrofauna (large polycheates, oligocheates, ophiuroids) were restricted to the sites below the OMZ
329 at St. 9 (770 m) and St. 10 (1024 m), where deep waters were oxygenated. However, small snails (~ 1
330 cm) were observed at St. 8 (407 m).
331

332 **3.3 Geochemical parameters in MUC cores**

333 Porewater and solid phase geochemistry of sediments retrieved by the MUC cores are shown in Fig. 2.
334 Surface sediment (0-0.5 cmbsf) POC content increased along the continental shelf from 1.6 wt % at
335 the shallow St. 1 (70 m) to a maximum of 15 wt % at St. 8 (253 m). Surface POC content decreased
336 again with increasing water depth showing the lowest POC content at St. 10 (1024 m, 2 wt %). While
337 POC content showed more or less stable profiles throughout the sediment core at St. 1 (70 m, around 3
338 wt %), St. 9 (770 m, around 4 wt %), and St. 10 (1024 m, around 3 wt %), POC content was stable
339 only in the upper ~ 10 cmbsf at St. 4 (150 m, around 10 wt %) and St. 6 (253 m, around 15 wt %),
340 followed by a decrease until the deepest sampled depth (2 wt % and 9 wt %, respectively). At St. 8
341 (407 m), POC content increased with sediment depth below 3 cmbsf (from 4 wt % to 9 wt %), which
342 consisted of dense clay (see above). In the upper 3 cmbsf, POC decreased from ~ 7 wt % to ~ 4 wt %,
343 which was the sediment layer with a more fluffy appearance.
344 The sediment surface C/N ratio was lowest at St. 1 (70 m, 6.2) and increased along the continental
345 shelf showing the highest surface C/N ratio at St. 10 (1024 m, 11). St. 8 (407 m) was exceptional, as it
346 showed slightly lower surface C/N ratio (8) as at St. 6 (253 m, 9). St. 8 (407 m) was also the only site
347 showing an increase of 4 units in the upper 0-5 cmbsf, followed by stable ratios around 12 throughout
348 the rest of the core. St. 1 and 4 (70 and 145 m) showed shallower increases in C/N ratio in the upper ~
349 2 cmbsf and upper 1 cmbsf, respectively, followed by stable ratios around 10 until the bottom of the
350 core. At St. 9 and 10 (770 and 1024 m), C/N ratios ranged around 11 and 12, respectively.
351 The highest increase in methane concentration was observed at St. 1 (70 m). Here, methane increased
352 linearly from the surface (1 µM) to the bottom of the core (100 µM). All other stations showed either
353 no clear trend (St. 4= 145 m) or only slight methane increases with depth. At St. 9 (770 m), even a
354 decrease in methane concentration was observed from the surface to the bottom of core.

Besides St. 1 (70 m), which showed a strong decrease in sulfate (SO_4^{2-}) concentration with depth from about 28 mM at the top to about 9 mM at the bottom of the core (43 cmbsf), all other stations showed SO_4^{2-} concentrations > 25 mM throughout the cores. At St. 4, 6 and 9 (145, 253, 770 m), SO_4^{2-} showed very slight decrease with depth from about 28 mM at the top to about 25 mM at the bottom of the core. Porewater SO_4^{2-} concentrations were stable around 28 mM throughout the core at St. 8 and 10 (407 and 1024 m).

Dissolved inorganic carbon (DIC) concentration increased with depth at St. 1- 6 (70 -253 m). St. 1 (70 m) showed the steepest increase with depth, showing the lowest DIC concentration at the top (2.3 mM) and the highest at the deepest sampled depth (21.6 mM). At St. 4 (153 m), maximum concentration was reached at ~ 23 cmbsf with 4 mM. St. 6 (253 m) showed maximum concentration at the deepest sampled depth with 9 mM. St. 8 and 9 (407 and 770 m) showed stable DIC concentrations around 2.3 mM throughout the core. No DIC data was available for St. 10 (1024 m).

3.4 Net methanogenesis and gross sulfate reduction in MUC cores

Maximum net methanogenesis rates (Fig. 2) were detected at St. 1 (70 m, 1.1 ±0.5 nmol cm^{-3} d^{-1}, 20-25 cmbsf) and St. 6 (253 m, 1.3 ±0.65 nmol cm^{-3} d^{-1}, 25-30 cmbsf). At all other stations, methanogenesis was mostly below 0.5 nmol cm^{-3} d^{-1} throughout the cores. St. 8 (407 m) showed methanogenesis activity only in the top 10 cmbsf with the maximum at 5-10 cmbsf (0.2 ±0.5 nmol cm^{-3} d^{-1}). At St. 9 and 10 (770 and 1024 m), maximum methanogenesis activity was found in the surface layer (0-5 cmbsf) with 0.3 ±0.4 nmol cm^{-3} d^{-1} and 0.4 ±0.6 nmol cm^{-3} d^{-1}, respectively. St. 10 (1024 m) also showed high average methanogenesis at 10-15 cmbsf (1.5 ±2.5 nmol cm^{-3} d^{-1}), which was caused by a single high replicate (4.3 nmol cm^{-3} d^{-1}). In the following, e.g., integration of rates, we will exclude this single high replicate, which will be further elaborated in the discussion.

At all stations beside St. 9 (770 m), sulfate reduction activity was highest in the 0-1 cmbsf horizon, followed by a sharp decrease in activity of 20-90% in the subsequent 1-2 cmbsf horizon. Highest measured rates at 0-1 cmbsf were observed at St. 4 (145 m, 290 nmol cm^{-3} d^{-1}), followed by St. 1 (70 m, 270 nmol cm^{-3} d^{-1}). Surface (0-1 cmbsf) sulfate reduction activity decreased from St. 4 (145 m) to

St. 8 (407 m) with concomitant increase in water depth. St. 9 (770 m) was the only site without a surface sulfate reduction maximum. Here, highest rates were found at 7 cmbsf (11.2 nmol cm^{-3} d^{-1}). St. 6, 8 and 9 (253, 407, and 770 m) showed a second but smaller maximum of sulfate reduction activity. At St. 6 (253 m), this second maximum was situated at 20.5 cmbsf (6.2 nmol cm^{-3} d^{-1}). St. 8 and 9 (407 and 770 m) showed additional maxima at 4.5 cmbsf (3.1 nmol cm^{-3} d^{-1}) and 2.5 cmbsf (1.5 nmol cm^{-3} d^{-1}), respectively. At St. 9 (770 m), sulfate reduction activity was not detectable at most depth > 10 cmbsf. At St.10 (1024 m), no sulfate reduction activity was detectable throughout the entire core. At St. 9 and 10 (770 and 1024 m) we cannot exclude that sulfate reduction was present but undetectable due to long, unfrozen storage of the samples (see 2.7).

Figure 3 shows an overview of integrated methanogenesis and sulfate reduction rates (over the upper 0-25 cm) along the depth transect on the Peruvian margin. Highest integrated surface methanogenesis activity was detected on the shelf (70, 145 and 253 m) with 0.1 ±0.03 mmol m^{-2} d^{-1}, 0.06 ±0.02 mmol m^{-2} d^{-1}, and 0.07 ±0.01 mmol m^{-2} d^{-1}, respectively. St. 8 (407 m) revealed the lowest integrated methanogenesis rate of all sites (0.02 ±0.00 mmol m^{-2} d^{-1}). St. 9 (770 m) and St. 10 (1024 m) showed integrated methanogenesis activity around 0.03 ±0.02 mmol m^{-2} d^{-1}, respectively.

Integrated sulfate reduction activity decreased along the continental margin with increasing water depth, revealing the highest activity at the St. 1 (70 m, 4.7 mmol m^{-2} d^{-1}) and the lowest activity at St. 9 (770 m, 0.2 mmol m^{-2} d^{-1}). Please note again, that integrated sulfate reduction rates are probably underestimated due to long, unfrozen storage of the samples (see 2.7).

3.5 Potential competitive and non-competitive methanogenesis in sediment slurries from MUC cores

Results from the sediment slurry experiments, in which we added either the sulfate reduction inhibitor molybdate, the non-competitive substrate methanol, or no additives (control), are shown in Fig. 4. During the first phase of incubation, all three treatments showed rates within the same order of magnitude. Nevertheless, potential methanogenesis rates were significantly higher ($p < 0.05$) in all treatments in the shallow sediment horizon (0-5 cmbsf) compared to the deep horizon (20-25 cmbsf).

In addition, potential methanogenesis was always significantly higher in the molybdate and methanol treatment compared to the control.

During the second phase of the incubation (day 8-23), potential methanogenesis showed a different pattern. Rates in the methanol treatment were 350 and 4 times higher compared to the control and molybdate treatment in the 0-5 cm horizon and the 20-25 cm horizon, respectively ($p < 0.05$). Control and molybdate treatments showed no significant difference ($p > 0.05$) in the shallow and deep horizon.

3.6 Geochemical parameters and gross hydrogenotrophic methanogenesis activity in gravity cores

At the shallow St. 1 (78 m), POC concentration slightly decreased with depth, from ~4 wt % at the surface to about 2-3 wt % at the bottom of the core (385 cmbsf, Fig. 5). At St. 8 (407 m), POC concentrations were slightly higher with values ranging around 8-9 wt % in the upper 120 cmbsf, and then decreasing with depth. The C/N ratio at St. 1 (78 m) remained around 10 throughout the core, while it showed slightly higher values around 12 throughout the core at St. 8 (407 m).

At St. 1 (78 m), the methane concentration increased with depth from 0.1 mM at the surface to the highest measured concentration at 165 cmbsf (~5 mM), followed by a decrease to ~ 2 mM at 198 cmbsf. Methane concentration stayed around 2 mM until the deepest measured depth (385 cmbsf). Methane concentrations at St. 8 (407 m) ranged from 14 to 17 µM in the upper 120 cmbsf, then increased to a maximum of 36 µM at 180 cmbsf, followed by a decrease to 28 µM at the deepest sampled depth (195 cmbsf).

SO_4^{2-} concentration at St. 1 (78 m) decreased with depth with the highest concentration (10 mM) at the shallowest measured sediment depth (33 cmbsf) and the lowest concentration at 350 cmbsf (0.16 mM). At St. 8 (407 m), SO_4^{2-} concentration decreased slightly from ~28 mM at the shallowest measured sediment depth (20 cmbsf) to ~24 mM at 145 cmbsf, followed by stable concentrations around 25 mM until the bottom of the core.

DIC concentrations were 5-8 times higher at St. 1 (78 m) compared to St. 8 (407 m) and increased with sediment depth from ~21 mM at 33 cmbsf to ~39 mM at 385 cmbsf. DIC concentrations at St. 8

436 (407 m) could only be measured at distinct sediment depths due to limited amounts of porewater but
437 still revealed a slight increase with sediment depth (from ~3 mM to ~5 mM).
438 Hydrogenotrophic methanogenesis at St. 1 (78 m) was present but low below 66 cmbsf until it reached
439 a peak between 300 and 400 cmbsf (0.7 nmol cm^{-3} d^{-1}). In contrast, no hydrogenotrophic
440 methanogenesis activity was detected at St. 8 (407 m).
441

442 **4. Discussion**

443 **4.1 Concurrent activity of methanogenesis and sulfate reduction in surface sediments**

444 Before we discuss the distribution of methanogenesis in the collected sediment cores, it has to be
445 pointed out that the top soft sediment layer (ca. 0-20 cm) of gravity cores is often disturbed or even
446 lost during the coring procedure. Hence, surface parameters in the gravity cores should not be directly
447 compared to the respective depth layers in MUC cores. According to this likely offset, we will use the
448 term "surface methanogenesis/sediments" when referring to MUC cores and "deep
449 methanogenesis/sediments" when referring to gravity cores.
450 We would further like the reader to keep in mind that we will compare two different types of rate
451 determinations: radiotracer incubations of undisturbed sediments (deep hydrogenotrophic
452 methanogenesis, surface sulfate reduction) and sediment slurry incubations (surface total
453 methanogenesis). While the first method preserves the natural heterogeneity of the sediment, the latter
454 homogenizes and dilutes sediment ingredients and organisms, which could have both negative and
455 positive effects on the natural activity. As we are mainly interested in the vertical distribution of these
456 processes within the sediment, these comparisons are justifiable.
457 In the present study, methanogenesis and sulfate reduction co-occurred in surface sediments along the
458 entire depth transect (70-1024 m) on the Peruvian margin (12°S). Methanogenesis activity was
459 detected in sediment layers that revealed high porewater sulfate concentrations and sulfate reduction
460 activity (besides St. 10, where sulfate reduction was undetectable). Even though absolute sulfate
461 reduction rates were most likely underestimated, we trust relative distribution pattern in the sediment
462 and along the continental margin.

As the competition between methanogens and sulfate reducers for H_2 and acetate was probably never relieved, the detected surface methanogenesis was most likely based on non-competitive substrates such as methanol or methylated compounds including methylated amines or methylated sulfides (Oremland & Polcin, 1982; Oremland & Taylor, 1978; Kiene et al., 1986). Likewise, in a study off Chile (0-6 cm sediment depth, 87 m water depth), surface methanogenesis was found to be coupled to the non-competitive substrate trimethylamine, and not to CO_2/H_2 or acetate, in sediments where sulfate and sulfate reduction was abundant (Ferdelman et al., 1997).

Non-competitive substrate utilization by methanogens in the present study was further confirmed by a significant increase of potential methanogenesis after the addition of methanol to sediment slurries from St. 1 (70 m) (Fig. 4 B). The delayed response of methanogenesis after methanol addition (Supplement, Fig. S1), however, suggests that the present microbial methanogenic community was not primarily feeding on methanol. Potentially, other non-competitive substrates like dimethyl sulfides were utilized predominantly. While most methylotrophic methanogens are able to use both methanol and methylated amines, growth on dimethyl sulfide appears to be restricted to only a few methylotrophic species (Oremland et al., 1989). Dimethyl sulfides could have accumulated during the long storage time (~ 6 months) before experimentation. Even though methylated sulfur compounds (e.g., dimethyl sulfide or methanthiol) are mainly produced by organisms in the marine photic zone (e.g., Andreae & Raemdonck 1983), it was recently postulated that these compounds may also be generated through nucleophilic attack by sulfide on methyl groups in the sedimentary organic matter (Mitterer, 2010). As sulfate reduction was a predominant process in the sediment, it could have delivered sufficient sulfide to produce methylated sulfur compounds. Consequently, results from the sediment slurry experiments might not reflect the activity of the in situ methanogenic community as we cannot exclude community shifts as a response to the availability of alternative substrates that were produced during the long storage.

The utilization of the competitive substrates H_2 and acetate by the methanogens probably only occurs when sulfate reducers are inhibited. Accordingly, potential methanogenesis rates in the molybdate treatment of the sediment slurry experiment were significantly higher in the two studied horizons (0-5 and 20-25 cmbsf) compared to the controls during the first phase of the incubation (day 0-5),

491 indicating the usage of competitive substrate facilitated by the inhibition of sulfate reduction.
492 However, in the second phase (day 8-23) of the incubation, rates were much lower in both the control
493 and molybdate treatment and did not show significant differences in both horizons ($p>0.05$). In this
494 second phase, methane production might have slowed down due to depletion of electron donors.
495 Hydrogenotrophic methanogenesis in the gravity core from St. 1 (78 m) showed no activity at depths
496 where porewater sulfate concentrations were >0.7 mM. Instead activity peaked where porewater
497 sulfate was lowest (0.16 mM at 350 cmbsf), supporting the above conclusions regarding competition
498 within the sulfate zone. The observation that sulfate was never completely depleted in the porewater
499 until the bottom of the gravity core, in combination with an increase of iron (II) in the porewater at
500 depths > 200 cmbsf (data not shown), hint to the presence of a cryptic sulfur cycle that is responsible
501 for deep formation of sulfate (Holmkvist et al., 2011; Treude et al., 2014) .
502 In comparison, surface net methanogenesis activity along the Peruvian margin was similar to activities
503 found off Chile at 87 m water depth (0-0.6 nmol cm^{-3} d^{-1}) (Ferdelman et al., 1997). The slightly higher
504 rates determined in our study (St.1= 70 m; 0.4-1.7 nmol cm^{-3} d^{-1}) could be related to different
505 approaches, as our rates represent the sum of net methanogenesis from all available substrates in the
506 sediment, while rates off Chile were based only on CO_2, acetate, and trimethylamine utilization.
507 Hence, total methanogenesis could have been easily underestimated, if methanogenesis was supplied
508 by other substrates, which is not unlikely, as methylotrophic methanogens, which are able to use
509 methanol or methylated amines, were the dominant type of methanogens in these sediments
510 (Ferdelman et al., 1997). Interestingly, the authors detected a high number of acetogens, implying that
511 acetogenesis competed for methylamines or other methylated compounds (Ferdelman et al., 1997). A
512 competition with acetogens for methylated substrates is conceivable for our study, but would require
513 further corroboration.
514

515 **4.2 Surface vs deep methanogenesis**

516 Maximum single net surface methanogenesis activities detected in our study (0.3-4.3 nmol cm^{-3} d^{-1})
517 were found to be at the very low end or even one order of magnitude lower than organic-rich, sulfate-
518 depleted sediments (9.8-37 nmol cm^{-3} d^{-1}, 0-40 cmbsf, Treude et al., 2005a, 10-17 nmol cm^{-3} d^{-1}, 0-30

519 cmbsf, Schmaljohann 1996, 100-300 nmol cm^{-3} d^{-1}, 0-30 cmbsf, Crill & Martens, 1983, 1986, 100-400
520 nmol cm^{-3} d^{-1},0-3 cmbsf, Alperin et al. 1992). To estimate the overall relevance of surface
521 methanogenesis within the sulfate zone compared to deep methane production, we estimated the deep
522 methane production in our study and compiled an overview of published deep methane production
523 data from the sulfate-free zone of organic-rich sediments (Table 2). For this comparison, the deep
524 methane production was assumed to equal the flux of methane into the sulfate-methane-transition zone
525 (SMTZ), where it is consumed by anaerobic oxidation of methane (AOM). Within the SMTZ, both
526 sulfate and methane are depleted steeply as a result of AOM, thus dividing the sulfate-reducing zone
527 above from the methanogenic zone below. The SMTZ is the main niche for AOM in marine
528 sediments, acting as an important filter for upwards migrating methane (Knittel & Boetius, 2009). The
529 SMTZ can be found at decimeters to tens of meters below the seafloor, depending on the burial rate of
530 reactive organic matter, the depth of the methane production zone, and the flux of methane and sulfate
531 as well as their consumption rates (Knittel & Boetius, 2009).
532 In the present study, a SMTZ was only detected in the gravity core taken at St. 1 (78 m; Fig. 5), where
533 it was located between 66 and 99 cmbsf, i.e., below the penetration depth of the MUC cores. We
534 estimated a methane flux (= deep methane production) into the SMTZ (from 99 to 66 cmbsf)
535 according to Iversen & Jørgensen, (1993) using a seawater methane-diffusion coefficient from Schulz,
536 (2006) which was corrected for porosity resulting in a sediment-diffusion coefficient for methane of
537 $D_{s=}$ 1.325×10^{-5} cm^{-2} s^{-1} at 15 °C. The resulting deep methane production (0.8 mmol m^{-2} d^{-1}) was slightly
538 higher (ratio of 0.13, surface vs. deep) but still in the same magnitude as the integrated surface
539 methanogenesis at St. 1 (70 m; 0.1 mmol m^{-2} d^{-1}). Compared to a different study from the Peruvian
540 OMZ, the ratio between shallow (0.07 to 0.1 mmol m^{-2} d^{-1}, this study) vs. deep (8.9×10^{-8} to $2.2*10^{-7}$
541 mmol m^{-2} d^{-1}; Arning et al., 2012) methanogenesis on the shelf (150-250 m) was 3.2×10^{5} to 1.1×10^{6}.
542 Both examples highlight the significance of surface methanogenesis, especially on the Peruvian shelf.
543 On the lower Peruvian slope (~3800 m water depth), deep methanogenesis increased (up to 0.017
544 mmol m^{-2} d^{-1}; Arning et al., 2012). In contrast, surface methanogenesis at the deeper St. 10 (1024 m)
545 was lower (0.02 mmol m^{-2} d^{-1}) compared to the shelf indicating a decreasing relevance of surface
546 methanogenesis along the margin with increasing relevance of deep methanogenesis. The decrease of

surface methanogenesis with increasing water depth might be correlated to the decreasing organic carbon content and freshness in the sediment (Fig. 6), as further discussed in section 4.4.

In comparison with other organic-rich sediments (Table 2), surface methanogenesis off Peru was in the same order of magnitude as most reported deep methanogenesis (e.g., off Namibia, off Chile, Limfjorden). The only exception was Eckernförde Bay (Baltic Sea), where surface methanogenesis off Peru was less than 15% of deep methanogenesis. Eckernförde Bay has a water depth of only ~30 m with high carbon export, featuring extremely high methanogenesis activity below the SMTZ, causing supersaturation and methane gas ebullition (Whiticar, 2002; Treude et al., 2005a).

4.3 Potential consumption and emission of surface methane

Due to its closeness to the sediment-water interface, surface methanogenesis along the Peruvian margin could lead to methane emissions from the sediment into the water column. A short diffusion distance, especially in the top most sediment layers, might facilitate a partial escape of methane from consumption by microbes. As surface methanogenesis decreased with water depth (Fig. 3), the methane emission potential appears to be highest on the shelf. Sediment methane concentrations in the 0-2 sediment horizon of all sites along the margin were always higher than bottom-near water methane concentrations (~1.5 m above seafloor; Table 1, Fig. 2), hinting towards an efflux of methane from the sediment. However, more precise profiling of methane at the sediment-water interface would be necessary to confirm this hypothesis. Still, most of the sediment methane profiles suggest methane consumption close to the seafloor to some extent, which would reduce the amount of emitted methane (Fig. 2). AOM might act as an important methane filter at the sediment surface of the shelf stations, where anoxic conditions dominated, while aerobic oxidation might prevail at the deeper stations below the OMZ (St. 9 and 10). The presence of methane oxidation above the SMTZ of organic-rich sediments has been reported earlier (Treude et al., 2005a, 2005b), and could indeed be fueled by surface methanogenesis. An immediate oxidation of the produced methane would explain why sediment methane profiles did not necessarily correlate with peaks in surface methanogenesis (see, e.g., St 6, 253 m). The importance of AOM for the reduction of methane emissions from surface methanogenesis remains speculative, as explicit data is missing. On the basis of our findings, however,

574 we suggest to consider surface methanogenesis as a possible driver for AOM above the SMTZ in
575 earlier and future studies.
576
577 **4.4 Factors controlling methanogenesis along the Peruvian margin**
578 For this discussion, we excluded the high integrated methane production observed in one of the
579 replicates at station 10 (1024 m) as we do not think that the detected activity (0.23 mmol m^{-2} d^{-1}) is
580 representative for this deep site, especially as sediment POC content was lowest at station 10
581 compared to the other stations (<4%, Fig. 2). The outlier might have been caused by additional carbon
582 sources in the sediment, e.g., from fecal pellets or organic carbon released from dead infauna, thus
583 stimulating below-surface microbial activities during our incubations (Ziervogel et al., 2014; Bertics et
584 al., 2013).
585
586 **4.4.1 Oxygen**
587 Oxygen is an important controlling factor, as methanogenesis is an oxygen- and redox-sensitive
588 process (Oremland, 1988). Some methanogens can tolerate oxygen exposure for several hours before
589 they die, although no methane is produced in the presence of oxygen (Zinder, 1993).
590 Comparing integrated surface methanogenesis (over 0-25 cmbsf) from the shallowest to the deepest
591 station (Fig. 3), highest rates (> 0.05 mmol m^{-2} d^{-1}) were detected on the shelf (St. 1, 4 and 6=70, 145,
592 253 m), where oxygen concentrations were below detection (Fig.6), providing advantageous
593 conditions for methanogenesis, particularly at the very sediment surface, where normally aerobic
594 respiration dominates (Jørgensen, 2006). Below the OMZ, integrated methanogenesis decreased.
595 Bioturbating macrofauna and megafauna (e.g., mussels, polycheates, oligocheates) were observed at
596 these sites (St. 9 and 10, 770 and 1024 m) (Mosch et al. 2012), which could have transported oxygen
597 into deeper sediment layer (Orsi et al., 1996), thus leading to less reduced conditions (> -200 mV)
598 unsuitable for methanogens (Oremland, 1988). However, integrated methanogenesis was lowest at St.
599 8 (407 m), which still revealed anoxic bottom water. Thus, oxygen might just be advantageous but not
600 the driving factor for surface methanogenesis.
601

4.4.2 Organic matter

The most important factor controlling benthic methanogenesis activity is probably the POC content of the sediment, as it determines the substrate availability and variety, and can thus relieve the competitive situation between methanogens and sulfate reducers (Holmer & Kristensen, 1994; Treude et al., 2009). Consequently, high methanogenesis rates may be expected along the Peruvian margin at sites with high organic carbon load. However, integrated methanogenesis rates did not correlate with sediment POC content (Fig. 6). While POC content was increasing from St. 1 (70 m) to St. 6 (253 m), followed by a decrease until St. 10 (1024 m), integrated methanogenesis showed rather a decreasing trend with increasing water depth. This deviation from expectations might be caused by another factor, such as organic matter quality, i.e., freshness. Numerous studies have shown that the quality of the organic matter is important for the rate and magnitude of microbial organic matter degradation (Westrich & Berner, 1984; Canfield, 1994; Amon et al., 2001; Middelburg, 1989).
Integrated methanogenesis and C/N ratios (indicating the freshness of organic matter) were negatively correlated along the Peruvian margin (Fig. 6), suggesting that fresh, labile organic matter is advantageous for surface methanogenesis. As methanogens consume mostly short, monomeric substrates, they depend on other microbial groups to break down large organic macromolecules (Zinder, 1993). Hence, labile organic matter offers an important supply of methanogenic substrates. In agreement with this hypothesis, highest integrated methanogenesis rates were observed at St. 1 (70 m), which revealed the freshest organic matter (lowest C/N, Fig. 6) and the highest POC remineralization rates along the Peruvian margin (Dale et al., 2015). The degradation of organic matter within the water column was probably limited at St. 1 (70 m) due to anoxic conditions and high sedimentation rates (Dale et al., 2015); hence, labile organic matter accumulated at the seafloor, thereby increasing the benthic POC degradation and resulting in high substrate availability and variety for the methanogenic community.

Nevertheless, lowest methanogenesis rates were measured at St. 8 (407 m), which was neither the site of the highest C/N ratio, lowest POC content (Fig. 6), or the lowest POC mineralization (Dale et al., 2015). In this particular case, methanogenesis was most likely controlled by the sediment properties. Methanogenesis activity was undetectable below 10 cmbsf, which coincided with a very dense and

630 sticky clay layer. The POC profile at St. 8 (407 m) revealed lower concentrations in the upper 5 cmbsf,
631 followed by an increase with depth, suggesting that either the organic matter at this station was
632 resistant to microbial attack (indicated by the increase in C/N) or that microbes were not as
633 frequent/active in the dense clay layer as at the surface. Similarly, sulfate reduction and microbial
634 nitrogen fixation (Gier et al., 2015) showed very low activity at this site (Fig. 2).
635

636 **5. Conclusion**

637 The present study demonstrated that methanogenesis coincides with sulfate reduction in surface
638 sediments (< 30 cmbsf) along the Peruvian margin. The competition with sulfate reducers was
639 partially relieved due to the high load of organic carbon allowing both groups to show concurrent
640 activity through the utilization of non-competitive substrates by the methanogens.
641 The significance of surface methanogenesis was high on the shelf, where ratios between surface and
642 deep methanogenesis were around 0.13 (this study) or even as high as ~10^5 (compared to Arning et al.
643 2012), and decreased with increasing water depth. Accordingly, we assume that potential methane
644 emissions into the water column, indicated by a higher methane concentration at the sediment surface
645 compared to the bottom water, should be highest on the shelf, where surface methane production rates
646 were highest. Our results further hint towards a partial consumption of methane before reaching the
647 sediment-water interface, probably by anaerobic oxidation of methane (AOM). In this case, surface
648 methanogenesis might act as important supplier of methane for AOM above the SMTZ, which has
649 been largely overlooked previously.
650 We postulate that the dominant factor controlling surface methanogenesis is the availability of
651 (primarily labile) organic matter. The high load of organic carbon and resulting high organic carbon
652 mineralization rates secure the supply of methanogenic substrates, especially on the shelf, which
653 mitigates the competition between sulfate reducers and methanogens. Anoxic conditions in the
654 overlying water might be advantageous for the oxygen-sensitive process of methanogenesis, but does
655 not appear to primarily control benthic rates, as they change within the anoxic zones.

Interestingly, organic matter made available by bioturbating infauna (e.g., fecal pellets or dead organisms) could be an important additional factor facilitating methanogenesis in surface sediments. As shown in this study, methanogenesis rates vary strongly in bioturbated sediments below the OMZ, sometimes exceeding all other observed methanogenic rates.

Future studies should seek to (1) identify methanogens and their metabolic capabilities in surface sediments, (2) determine the direct interaction between surface methanogenesis and AOM, and (3) evaluate the effect of organic matter hot spots on total benthic surface methanogenesis in organic-rich sediments.

Acknowledgements

We thank the captain and crew of R.V. Meteor for field assistance. We thank A. Petersen, S. Kriwanek and S. Cherednichenko and the shipboard scientific party for field and laboratory assistance. For the geochemical analysis we want to thank B. Domeyer, A. Bleyer, U. Lomnitz, R. Suhrberg, S. Trinkler and V. Thoenissen. Additional thanks goes to G. Schuessler, P. Wefers, and S. Krause of the Treude working group for their laboratory assistance. We further thank the authorities of Peru for the permission to work in their territorial waters. This study is a contribution of the Sonderforschungsbereich 754 "Climate – Biogeochemistry Interactions in the Tropical Ocean" (www.sfb754.de), which is supported by the German Research Foundation. Further support came from the Cluster of Excellence "The Future Ocean" funded by the by the German Research Foundation.

Author contribution

J.M. and T.T. designed the experiments. J.M. carried out all methanogenesis experiments, T.T. conducted sulfate reduction measurements. Porewater measurements of MUC cores were coordinated by A.D. and S.S. J.M. prepared the manuscript with contributions of all co-authors.

References

Alperin, M.J., Blair, N.E., Albert, D.B., Hoehler, T.M. & Martens, C.S. (1992). Factors that control the stable isotopic composition of methane produced in an anoxic marine sediment. *Global Biogeochemical Cycles*. 6 (3). pp. 271–291.

Amon, R.M.W., Fitznar, H.-P. & Benner, R. (2001). Linkages among the bioreactivity, chemical composition, and diagenetic state of marine dissolved organic matter. *Limnology and Oceanography*. 46 (2). pp. 287–297.

Andreae, M.O. & Raemdonck, H. (1983). Dimethyl sulfide in the surface ocean and the marine atmosphere: a global view. *Science (New York, N.Y.)*. 221 (4612). pp. 744–747.

Arning, E.T., Van Berk, W. & Schulz, H.M. (2012). Quantitative geochemical modeling along a transect off Peru: Carbon cycling in time and space, and the triggering factors for carbon loss and storage. *Global Biogeochemical Cycles*. 26 (4). pp. 1–18.

Bange, H.W., Bartell, U.H., Rapsomanikis, S. & Andreae, M.O. (1994). Methane in the Baltic and North Seas and a reassessment of the marine emissions of methane. *Global Biogeochemical Cycles*. 8 (4). pp. 465–480.

Bange, H.W., Hansen, H.P., Malien, F., Laß, K., Karstensen, J., Petereit, C., Friedrichs, G. & Dale, A. (2011). Boknis Eck Time Series Station (SW Baltic Sea): Measurements from 1957 to 2010. *LOICZ-Affiliated Activities*. Inprint 20. pp. 16–22.

Bertics, V.J., Löscher, C.R., Salonen, I., Dale, A.W., Gier, J., Schmitz, R.A. & Treude, T. (2013). Occurrence of benthic microbial nitrogen fixation coupled to sulfate reduction in the seasonally hypoxic Eckernförde Bay, Baltic Sea. *Biogeosciences*. 10 (3). pp. 1243–1258.

Buckley, D.H., Baumgartner, L.K. & Visscher, P.T. (2008). Vertical distribution of methane metabolism in microbial mats of the Great Sippewissett Salt Marsh. *Environmental microbiology*. 10 (4). pp. 967–77.

Canfield, D.E. (1994). Factors influencing organic carbon preservation in marine sediments. *Chemical geology*. 114 (93). pp. 315–329.

Crill, P. & Martens, C. (1983). Spatial and temporal fluctuations of methane production in anoxic coastal marine sediments. *Limnology and Oceanography*. 28. pp. 1117–1130.

Crill, P.M. & Martens, C.S. (1986). Methane production from bicarbonate and acetate in an anoxic marine sediment. *Geochimica et Cosmochimica Acta*. 50. pp. 2089–2097.

Dale, A.W., Sommer, S., Lomnitz, U., Montes, I., Treude, T., Liebetrau, V., Gier, J., Hensen, C., Dengler, M., Stolpovsky, K., Bryant, L.D. & Wallmann, K. (2015). Organic carbon production, mineralisation and preservation on the Peruvian margin. *Biogeosciences*. 12. pp. 1537–1559.

Dimitrov, L. (2002). Mud volcanoes – the most important pathways for degassing deeply buried sediments. *Earth Science Review*. 59. pp. 49–76.

Donnelly, M.I. & Dagley, S. (1980). Production of Methanol from Aromatic Acids by Pseudomonas putida. *Journal of bacteriology*. 142 (3). pp. 916–924.

718 Ferdelman, T.G., Lee, C., Pantoja, S., Harder, J., Bebout, B.M. & Fossing, H. (1997). Sulfate
719 reduction and methanogenesis in a Thioploca-dominated sediment off the coast of Chile.
720 *Geochimica et Cosmochimica Acta*. 61 (15). pp. 3065–3079.

721 Fuenzalida, R., Schneider, W., Garcés-Vargas, J., Bravo, L. & Lange, C. (2009). Vertical and
722 horizontal extension of the oxygen minimum zone in the eastern South Pacific Ocean. *Deep-Sea*
723 *Research Part II: Topical Studies in Oceanography*. 56. pp. 992–1003.

724 Gallardo, V.A. (1977). Large benthic microbial communities in sulphide biota under Peru-Chile
725 subsurface countercurrent. *Nature*. 268. pp. 331–332.

726 Gier, J., Sommer, S., Löscher, C.R., Dale, A.W., Schmitz, R.A. & Treude, T. (2015). Nitrogen fixation
727 in sediments along a depth transect through the Peruvian oxygen minimum zone. *Biogeosciences*
728 *Discussions*. 12 (17). pp. 14401–14440.

729 Hines, M.E. & Buck, J.D. (1982). Distribution of methanogenic and sulfate-reducing bacteria in near-
730 shore marine sediments. *Applied and environmental microbiology*. 43 (2). pp. 447–453.

731 Holmer, M. & Kristensen, E. (1994). Coexistence of sulfate reduction and methane production in an
732 organic-rich sediment. *Marine Ecology Progress Series*. 107. pp. 177–184.

733 Holmkvist, L., Ferdelman, T.G. & Jørgensen, B.B. (2011). A cryptic sulfur cycle driven by iron in the
734 methane zone of marine sediment (Aarhus Bay, Denmark). *Geochimica et Cosmochimica Acta*.
735 75 (12). pp. 3581–3599.

736 IPCC (2014). *Climate Change 2014: Synthesis Report.Contribution of Working Groups I, II and III to*
737 *the Fifth Assessment Report of the Intergovernmental Panel on Climate Change*. T. core writing
738 Team, R. K. Pachauri, & L. A. Meyer (eds.). Geneva, Switzerland.

739 Iversen, N. & Jørgensen, B.B. (1993). Diffusion coefficients of sulfate and methane in marine
740 sediments: Influence of porosity. *Geochimica et Cosmochimica Acta*. 57 (3). pp. 571–578.

741 Jørgensen, B.B. (1978). A comparison of methods for the quantification of bacterial sulfate reduction
742 in coastal marine sediments: I. Measurements with radiotracer techniques. *Geomicrobiology*
743 *Journal*. 1. pp. 11–27.

744 Jørgensen, B.B. (2006). Bacteria and marine Biogeochemistry. In: H. D. Schulz & M. Zabel (eds.).
745 *Marine Geochemistry*. Berlin/Heidelberg: Springer-Verlag, pp. 173–207.

746 Jørgensen, B.B. (1977). The sulfur cycle of a coastal marine sediment (Limfjorden, Denmark).
747 *Limnology and Oceanography*. 22 (5). pp. 814–832.

748 Jørgensen, B.B. & Parkes, R.J. (2010). Role of sulfate reduction and methane production by organic
749 carbon degradation in eutrophic fjord sediments (Limfjorden, Denmark). *Limnology and*
750 *Oceanography*. 55 (3). pp. 1338–1352.

751 Judd, A., Davies, G., Wilson, J., Holmes, R., Baron, G. & Bryden, I. (1997). Contributions to
752 atmospheric methane by natural seepages on the UK continental shelf. *Marine Geology*. 137 (1-
753 2). pp. 165–189.

754 Kallmeyer, J., Ferdelman, T.G., Weber, A., Fossing, H. & Jørgensen, B.B. (2004). Evaluation of a
755 cold chromium distillation procedure for recovering very small amounts of radiolabeled sulfide
756 related to sulfate reduction measurements. *Limnology and Oceanography: Methods*. 2. pp. 171–
757 180.

Kamykowski, D. & Zentara, S. (1990). Hypoxia in the world ocean as recorded in the historical data set. *Deep-Sea Research*. 37 (12). pp. 1861–1874.

Kiene, R.P., Oremland, R.S., Catena, a, Miller, L.G. & Capone, D.G. (1986). Metabolism of reduced methylated sulfur compounds in anaerobic sediments and by a pure culture of an estuarine methanogen. *Applied and environmental microbiology*. 52 (5). pp. 1037–1045.

King, G.M., Klug, M.J. & Lovley, D.R. (1983). Metabolism of acetate, methanol, and methylated amines in intertidal sediments of lowes cove, maine. *Applied and environmental microbiology*. 45 (6). pp. 1848–1853.

Knittel, K. & Boetius, A. (2009). Anaerobic oxidation of methane: progress with an unknown process. *Annual review of microbiology*. 63. pp. 311–34.

Kristensen, E. (2000). Organic matter diagenesis at the oxic/anoxic interface in coastal marine sediments, with emphasis on the role of burrowing animals. *Hydrobiologia*. 426 (1). pp. 1–24.

Van Der Maarel, M.J.E.C. & Hansen, T. a. (1997). Dimethylsulfoniopropionate in anoxic intertidal sediments: A precursor of methanogenesis via dimethyl sulfide, methanethiol, and methiolpropionate. *Marine Geology*. 137 (1-2). pp. 5–12.

Middelburg, J.J. (1989). A simple rate model for organic matter decomposition in marine sediments. *Geochimica et Cosmochimica Acta*. 53 (7). pp. 1577–1581.

Mitterer, R.M. (2010). Methanogenesis and sulfate reduction in marine sediments: A new model. *Earth and Planetary Science Letters*. 295 (3-4). pp. 358–366.

Neill, a R., Grime, D.W. & Dawson, R.M. (1978). Conversion of choline methyl groups through trimethylamine into methane in the rumen. *The Biochemical journal*. 170 (3). pp. 529–535.

Niewöhner, C., Hensen, C., Kasten, S., Zabel, M. & Schulz, H.D. (1998). Deep sulfate reduction completely mediated by anaerobic oxidation in sediments of the upwelling area off Namibia. *Geochimica et Cosmochimica Acta*. 62 (3). pp. 455–464.

Oremland, R.S. (1988). Biogeochemistry of methanogenic bacteria. In: A. J. B. Zehnder (ed.). *Biology of Anaerobic Microorganisms*. New York: J. Wiley & Sons, pp. 641–705.

Oremland, R.S. & Capone, D.G. (1988). Use of specific inhibitors in biogeochemistry and microbial ecology. In: K. C. Marshall (ed.). *Advances in Microbial Ecology*. Advances in Microbial Ecology. Boston, MA: Springer US, pp. 285–383.

Oremland, R.S., Kiene, R.P., Mathrani, I., Whiticar, M.J. & Boone, D.R. (1989). Description of an estuarine methylotrophic methanogen which grows on dimethyl sulfide. *Applied and environmental microbiology*. 55 (4). pp. 994–1002.

Oremland, R.S., Marsh, L. & Desmarais, D.J. (1982). Methanogenesis in Big Soda Lake , Nevada : an Alkaline , Moderately Hypersaline Desert Lake. *Applied and environmental microbiology*. 43 (2). pp. 462–468.

Oremland, R.S. & Polcin, S. (1982). Methanogenesis and Sulfate Reduction : Competitive and Noncompetitive Substrates in Estuarine Sediments. *Applied and Environmental Microbiology*. 44 (6). pp. 1270–1276.

796 Oremland, R.S. & Taylor, B.F. (1978). Sulfate reduction and methanogenesis in marine sediments.
797 *Geochimica Cosmochimica Acta*. 42. pp. 209–214.

798 Orsi, T.H., Werner, F., Milkert, D., Anderson, a. L. & Bryant, W.R. (1996). Environmental overview
799 of Eckernförde Bay, northern Germany. *Geo-Marine Letters*. 16 (3). pp. 140–147.

800 Pennington, J.T., Mahoney, K.L., Kuwahara, V.S., Kolber, D.D., Calienes, R. & Chavez, F.P. (2006).
801 Primary production in the eastern tropical Pacific: A review. *Progress in Oceanography*. 69 (2-
802 4). pp. 285–317.

803 Reeburgh, W. (2007). Oceanic methane biogeochemistry. *Chemical Reviews*. 107. pp. 486–513.

804 Reimers, C.E. & Suess, E. (1983). The partitioning of organic carbon fluxes and sedimentary organic
805 matter decomposition rates in the ocean. *Marine Chemistry*. 13. pp. 141–168.

806 Røy, H., Weber, H.S., Tarpgaard, I.H., Ferdelman, T.G. & Jørgensen, B.B. (2014). Determination of
807 dissimilatory sulfate reduction rates in marine sediment via radioactive 35S tracer. *Limnology*
808 *and Oceanography: Methods*. 12. pp. 196–211.

809 Schink, B. & Zeikus, J.G. (1982). Microbial Ecology of Pectin Decomposition in Anoxic Lake
810 Sediments and in defined laboratory cultures of species prevalent in the lake sediment . The
811 turnover. *Journal of General Microbiology*. 128 (393-404). pp. 393–404.

812 Schmaljohann, R. (1996). Methane dynamics in the sediment and water column of Kiel Harbour
813 (Baltic Sea). *Marine Chemistry*. 131. pp. 263–273.

814 Schulz, H.D. (2006). Quantification of early diagenesis: dissolved constituents in marine pore water.
815 In: H. D. Schulz & M. Zabel (eds.). *Marine Geochemistry*. Berlin, Heidelberg: Springer Berlin
816 Heidelberg, pp. 75–124.

817 Seeberg-Elverfeldt, J., Schluter, M., Feseker, T. & Kolling, M. (2005). Rhizon sampling of porewaters
818 near the sediment-water interface of aquatic systems. *Limnology and Oceanography-Methods*. 3.
819 pp. 361–371.

820 Senior, E., Lindström, E.B., Banat, I.M. & Nedwell, D.B. (1982). Sulfate reduction and
821 methanogenesis in the sediment of a saltmarsh on the East coast of the United kingdom. *Applied*
822 *and environmental microbiology*. 43 (5). pp. 987–996.

823 Smetacek, V. (1985). The Annual Cycle of Kiel Bight Plankton: A Long-Term Analysis. *Estuaries*. 8
824 (June). pp. 145–157.

825 Thauer, R.K. (1998). Biochemistry of methanogenesis : a tribute to Marjory Stephenson.
826 *Microbiology*. 144. pp. 2377–2406.

827 Treude, T., Krause, S., Maltby, J., Dale, A.W., Coffin, R. & Hamdan, L.J. (2014). Sulfate reduction
828 and methane oxidation activity below the sulfate-methane transition zone in Alaskan Beaufort
829 Sea continental margin sediments: Implications for deep sulfur cycling. *Geochimica et*
830 *Cosmochimica Acta*. 144. pp. 217–237.

831 Treude, T., Krüger, M., Boetius, A. & Jørgensen, B.B. (2005a). Environmental control on anaerobic
832 oxidation of methane in the gassy sediments of Eckernförde Bay (German Baltic). *Limnology*
833 *and Oceanography*. 50 (6). pp. 1771–1786.

Treude, T., Niggemann, J., Kallmeyer, J., Wintersteller, P., Schubert, C.J., Boetius, A. & Jørgensen, B.B. (2005b). Anaerobic oxidation of methane and sulfate reduction along the Chilean continental margin. *Geochimica et Cosmochimica Acta*. 69 (11). pp. 2767–2779.

Treude, T., Smith, C.R., Wenzhöfer, F., Carney, E., Bernardino, A.F., Hannides, A.K., Krgüer, M. & Boetius, A. (2009). Biogeochemistry of a deep-sea whale fall: Sulfate reduction, sulfide efflux and methanogenesis. *Marine Ecology Progress Series*. 382. pp. 1–21.

Valentine, D.L., Blanton, D.C., Reeburgh, W.S. & Kastner, M. (2001). Water column methane oxidation adjacent to an area of active hydrate dissociation, Eel River Basin. *Geochimica et Cosmochimica Acta*. 65 (16). pp. 2633–2640.

Westrich, J.T. & Berner, R. a. (1984). The role of sedimentary organic matter in bacterial sulfate reduction: The G model tested. *Limnology and Oceanography*. 29 (2). pp. 236–249.

Wever, T.F. & Fiedler, H.M. (1995). Variability of acoustic turbidity in Eckernförde Bay (southwest Baltic Sea) related to the annual temperature cycle. *Marine Geology*. 125. pp. 21–27.

Whiticar, M.J. (2002). Diagenetic relationships of methanogenesis, nutrients, acoustic turbidity, pockmarks and freshwater seepages in Eckernförde Bay. *Marine Geology*. 182. pp. 29–53.

Whiticar, M.J. (1978). *Relationships of interstitial gases and fluids during early diagenesis in some marine sediments*.

Widdel, F. & Bak, F. (1992). Gram-Negative Mesophilic Sulfate-Reducing Bacteria. In: A. Balows, H. G. Trüper, M. Dworkin, W. Harder, & K.-H. Schleifer (eds.). *The Prokaryotes*. New York, NY: Springer New York, pp. 3352–3378.

Ziervogel, K., Joye, S.B. & Arnosti, C. (2014). Microbial enzymatic activity and secondary production in sediments affected by the sedimentation pulse following the Deepwater Horizon oil spill. *Deep-Sea Research Part II: Topical Studies in Oceanography*. pp. 1–8.

Zinder, S.H. (1993). Physiological ecology of methanogens. In: J. G. Ferry (ed.). *Methanogenesis*. New York, NY: Chapman & Hall, pp. 128–206.

866 **Figure Captions**

867

868 **Figure 1**: Location of sampling sites off Peru along the depth transect at 12° S. Source: Schlitzer, R.,
869 Ocean Data View, http://odv.awi.de, 2014

870 **Figure 2**: Profiles of particulate organic carbon (POC), C/N ratio, methane (CH_4), sulfate (SO_4^{2-}), DIC
871 (dissolved inorganic carbon), net methanogenesis (MG) rates and sulfate reduction (SR) rates in the
872 MUC cores along the depth transect. For MG, triplicates (symbols) and mean (solid line) are shown.
873 For SR, duplicates are shown. Data points from the overlaying water in the MUC core (OLW) are set
874 to 0 cm. Note deviant scale dimension for MG at St. 6 and for SR at St. 1 and 2.

875

876 **Figure 3**: Integrated methanogenesis and sulfate reduction rates (0-25 cm) along the depth transect.
877 For methanogenesis rates (black bars), average values are shown with standard deviation. Note for St.
878 10 a mean from two replicates is shown without standard deviation (pattern-filled bar) and the outlier
879 is shown separately (cross). For sulfate reduction rates (blue bars), means from two replicates are
880 shown without standard deviation.

881 **Figure 4**: Potential methanogenesis rates in sediment slurry experiments from the two sediment
882 intervals (0-5 cm and 20-25 cm) at St. 1 (70 m). The first phase of the incubation shows rates
883 calculated from day 0 to 5 (A), while the second phase of the incubation summarizes the rates from
884 day 8-23 (B). "Control" is the treatment with sulfate-rich (28 mM) artificial seawater medium, "plus
885 Mb" is the treatment with sulfate-rich artificial seawater medium plus molybdate (Mb, 22mM), and
886 "plus Meth" is defined as the treatment with sulfate-rich artificial seawater medium plus methanol
887 (Meth, 10 mM). Per treatment, average values are shown with standard deviation. Please note the
888 split-up in the diagram in part B and the different x-axis for methanogenesis

889

890 **Figure 5**: Profiles of particulate organic carbon (POC), C/N ratio, methane (CH_4), sulfate (SO_4^{2-}),
891 dissolved inorganic carbon (DIC), and hydrogenotrophic methanogenesis (MG) rates in the gravity
892 cores at two stations within the depth transect. For MG, triplicates (symbols) and mean (solid line) are
893 shown.

894

895 **Figure 6**: Bottom-near water methane (CH_4) and oxygen (O_2) concentrations along the depth transect
896 (above). Surface sediment particulate organic carbon (POC) content and C/N ratio together with
897 integrated methanogenesis (MG) rates (0-25 cmbsf) along the depth transect (below). For MG rates,
898 averages are shown with standard deviation beside St. 10, where a mean from two replicates is shown
899 (see text). Please note the secondary y-axis.

900

901

902

903 **Tables**

904 Table 1: Stations, instruments, chemical/physical parameters in the bottom-near water, and analyses
905 applied to samples along the depth transect on the Peruvian margin (12°S). For abbreviations see
906 footnote.

Station No	Instrument	Latitude (S)	Longitude (W)	Water depth (m)	O_2 (µM)	Temp. (°C)	CH_4 (nM)	Type of analysis
1	MUC 13	12°13.492	77°10.511	70				All
	MUC 38	12°13.517	77°10.084	70				SE
	GC 8	12°14.500	77°9.611	78				GC-All
	CTD 9	12°13.535	77°10.522	73	bdl	14	38.6	WC
4	MUC 10	12°18.704	77°17.790	145				All
	CTD 14	12°18.697	77°18.004	145	bdl	13.4	24.4	WC
6	MUC 5	12°23.321	77°24.176	253				Gas+PW
	MUC 6	12°23.322	77°24.181	253				nMG
	CTD 6	12°24.904	77°26.314	305	bdl	12	79.6	WC
8	MUC 23	12°27.198	77°29.497	407				Gas+ PW
	MUC 24	12°27.197	77°29.497	407				nMG
	GC 3	12°27.192	77°29.491	407				GC-All
	CTD 37	12°29.502	77°29.502	407	bdl	10.6	7.3	WC
9	MUC 17	12°31.374	77°35.183	770				Gas+ PW
	MUC 18	12°31.373	77°35.184	770				nMG
	CTD 27	12°31.327	77°35.265	770	19	5.5	8.4	WC
10	MUC 28	12°35.377	77°40.975	1024				Gas+ PW
	MUC 29	12°35.377	77°40.976	1024				nMG
	CTD 11	12°34.863	77°38.954	1010	53	4.4	3.9	WC

907 MUC = multicorer, GC= gravity corer, CTD = CTD/Rosette, bdl= below detection limit (5µM), All = methane
908 gas analysis, porewater analysis, net methanogenesis analysis, SE = slurry experiment, GC-All= analysis for
909 gravity cores including methane gas anaylsis, porewater analysis, hydrogenotrophic methanogenesis analysis,
910 WC= Water column analyses, Gas = methane gas analysis, PW= porewater analysis, nMG= net methanogenesis
911 analysis,
912

Table 2: Comparison of deep methanogenesis in organic-rich sediments from different regions with surface methanogenesis (0.02-0.1 mmol m^{-2} d^{-1}) determined in the present study. The ratio range was achieved by dividing the lowest surface by the highest deep and the highest surface by the lowest deep methanogenic activity, respectively.

	Water Depth (m)	**Depth of SMTZ** (mbsf)	**Methane flux into the SMTZ = integrated deep methanogenesis** (mmol m^{-2} d^{-1})	**Ratio between surface methanogenesis (present study) and deep methanogenesis**	**Reference**
Namibia (SE Atlantic)	1312-2060	3-10	0.07-0.15	0.13-1.43	Niewöhner et al., (1998)
Eckernförde Bay (SW Baltic Sea)	25-28	0.5-1.5	0.66-1.88	0.01-0.15	Treude et al., (2005a)
Chile (SE Pacific)	797-2746	3-4	0.068-0.13	0.15-1.47	Treude et al., (2005b)
Limfjorden (North Sea)	7-10	1-1.5	0.076	0.03-1.32	Jørgensen & Parkes, (2010)
Peru (SE Pacific)	150-3819	2-50	2.2×10^{-7}-0.017	1.18-4.55×10^{5}	Arning et al., (2012)
Peru (SE Pacific)	70-1024	0.7-1	0.8	0.03-0.13	present study

914

915

916

Figures

Figure 1

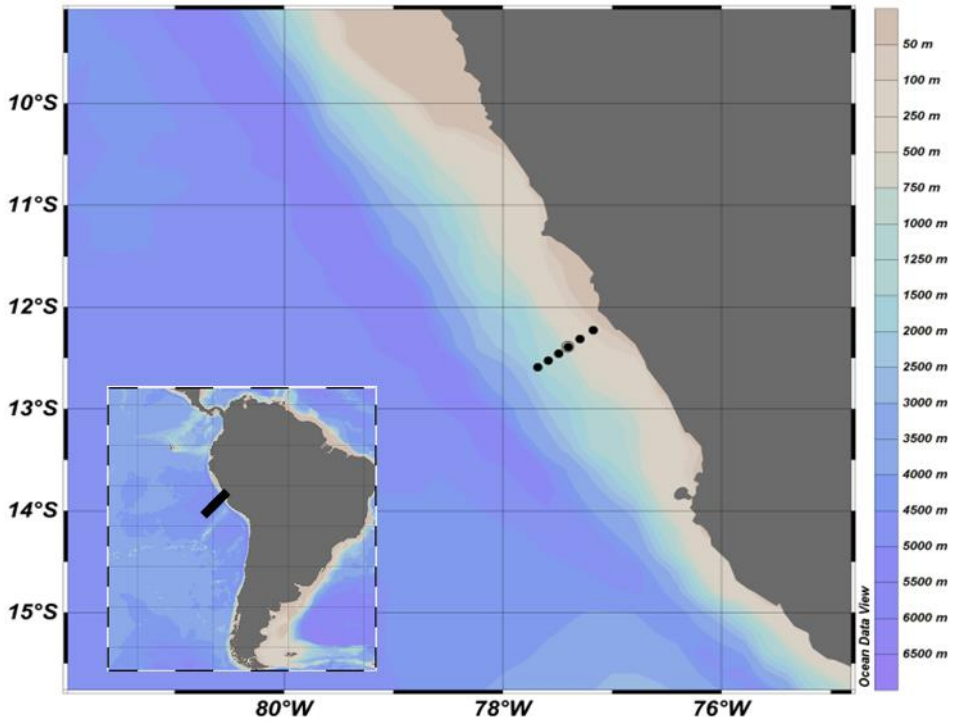

Figure 2

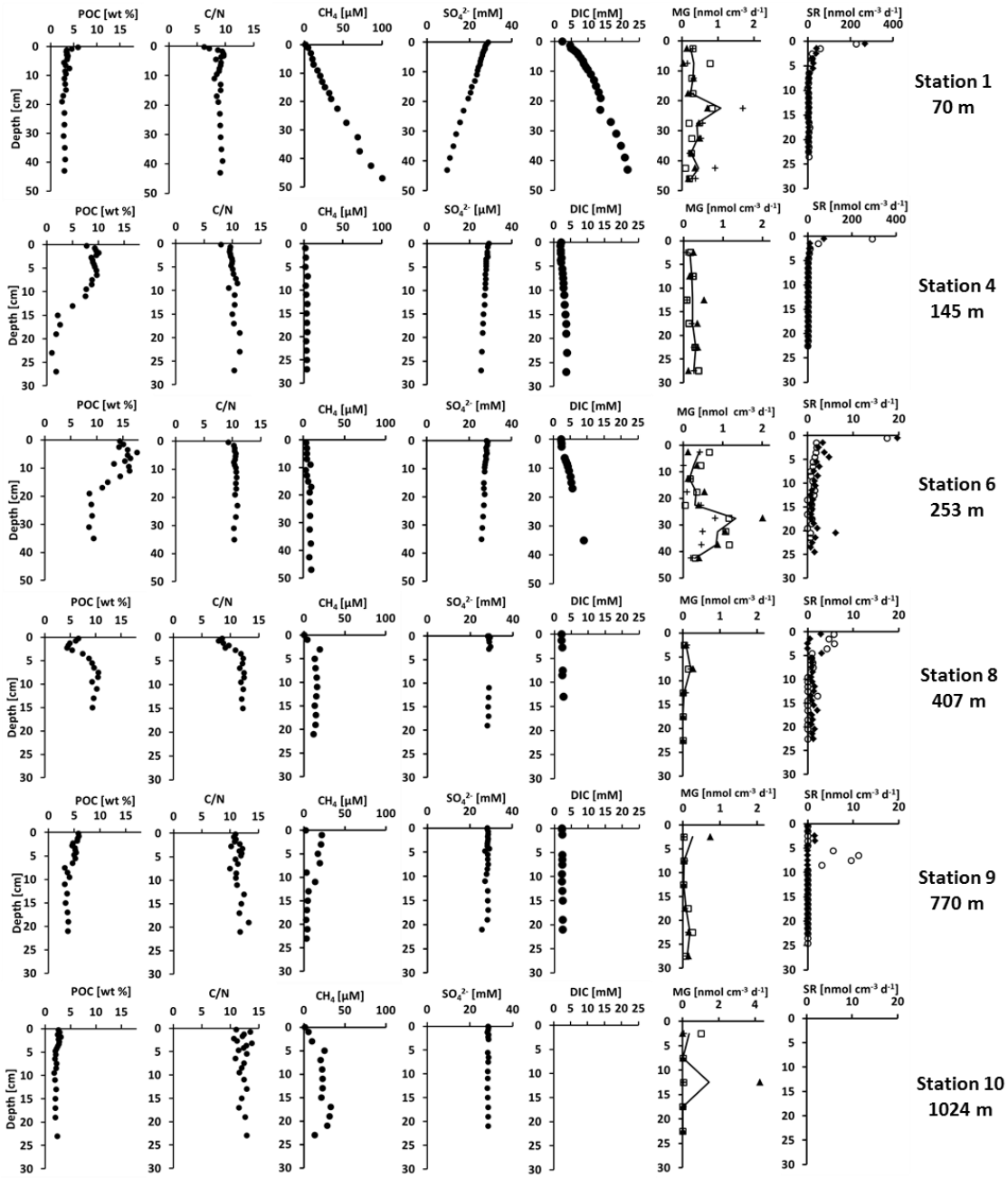
POC [wt %]
C/N
CH4 [µM]
SO4 2- [mM]
DIC [mM]
MG [nmol cm-3 d-1]
SR [nmol cm-3 d-1]
Depth [cm]
Station 1
70 m
Station 4
145 m
Station 6
253 m
Station 8
407 m
Station 9
770 m
Station 10
1024 m

Figure 3

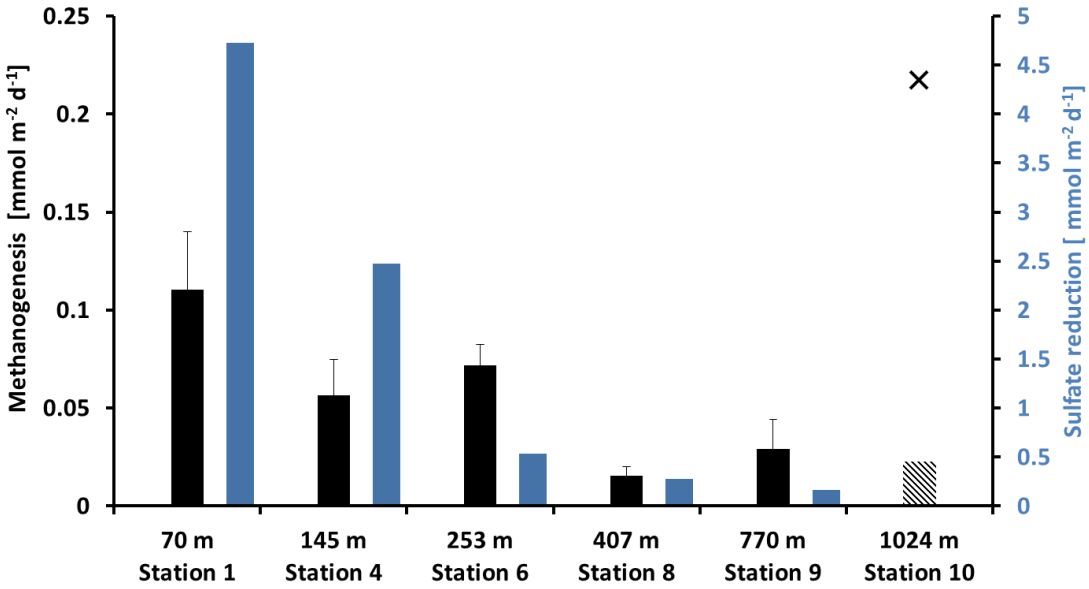
Methanogenesis [mmol m-2 d-1]
0.25
0.2
0.15
0.1
0.05
0
Sulfate reduction [mmol m-2 d-1]
5
4.5
4
3.5
3
2.5
2
1.5
1
0.5
0
70 m
Station 1
145 m
Station 4
253 m
Station 6
407 m
Station 8
770 m
Station 9
1024 m
Station 10

Figure 4

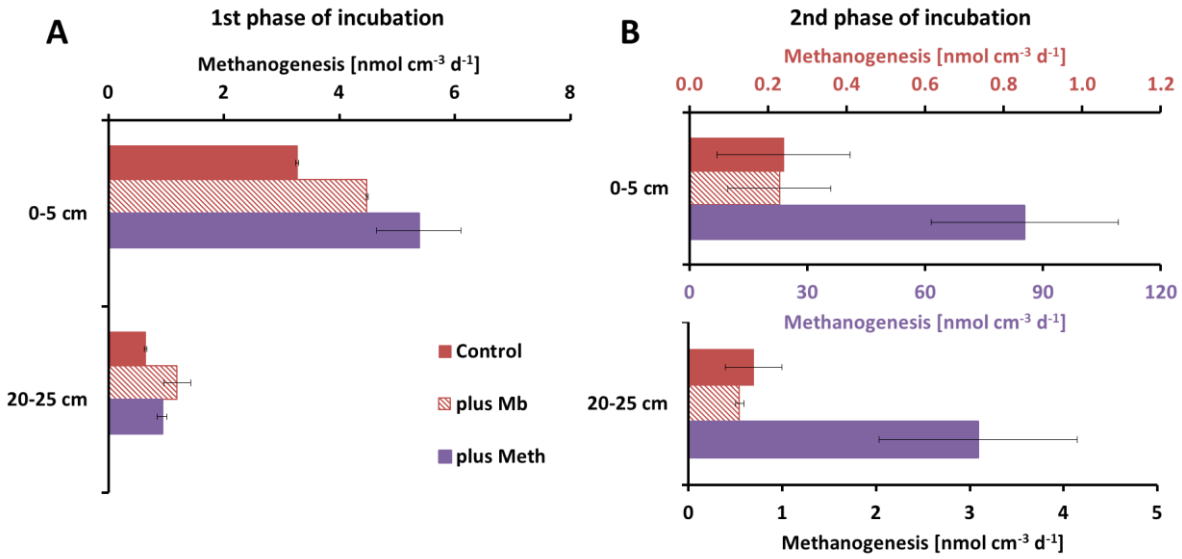
A
1st phase of incubation
Methanogenesis [nmol cm-3 d-1]
0
2
4
6
8
0-5 cm
20-25 cm
Control
plus Mb
plus Meth
B
2nd phase of incubation
Methanogenesis [nmol cm-3 d-1]
0.0
0.2
0.4
0.6
0.8
1.0
1.2
0-5 cm
0
30
60
90
120
Methanogenesis [nmol cm-3 d-1]
20-25 cm
0
1
2
3
4
5
Methanogenesis [nmol cm-3 d-1]

Figure 5

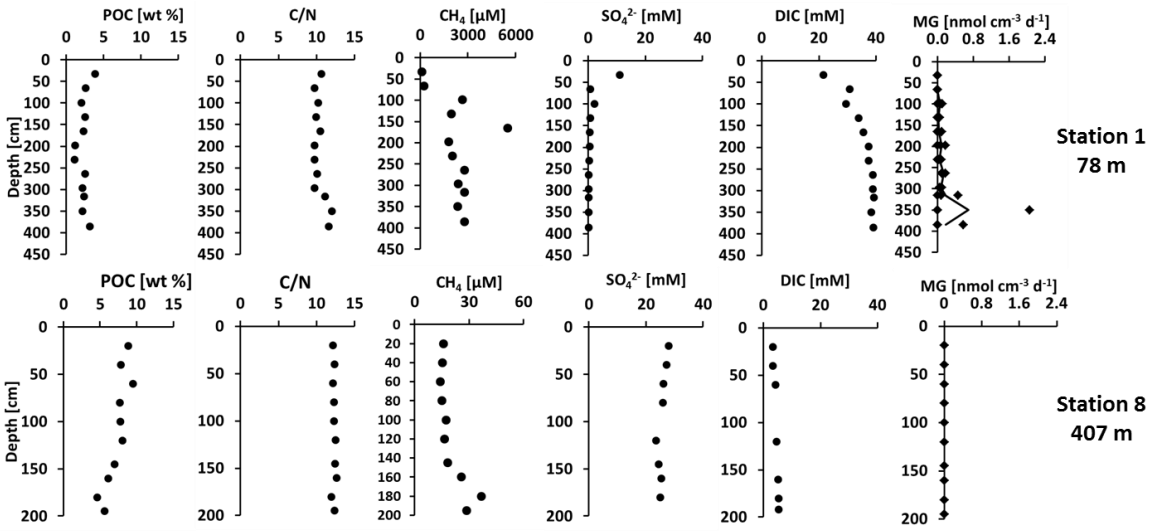
POC [wt %]
C/N
CH4 [µM]
SO4 2- [mM]
DIC [mM]
MG [nmol cm-3 d-1]
Depth [cm]
Station 1
78 m
Station 8
407 m

Figure 6

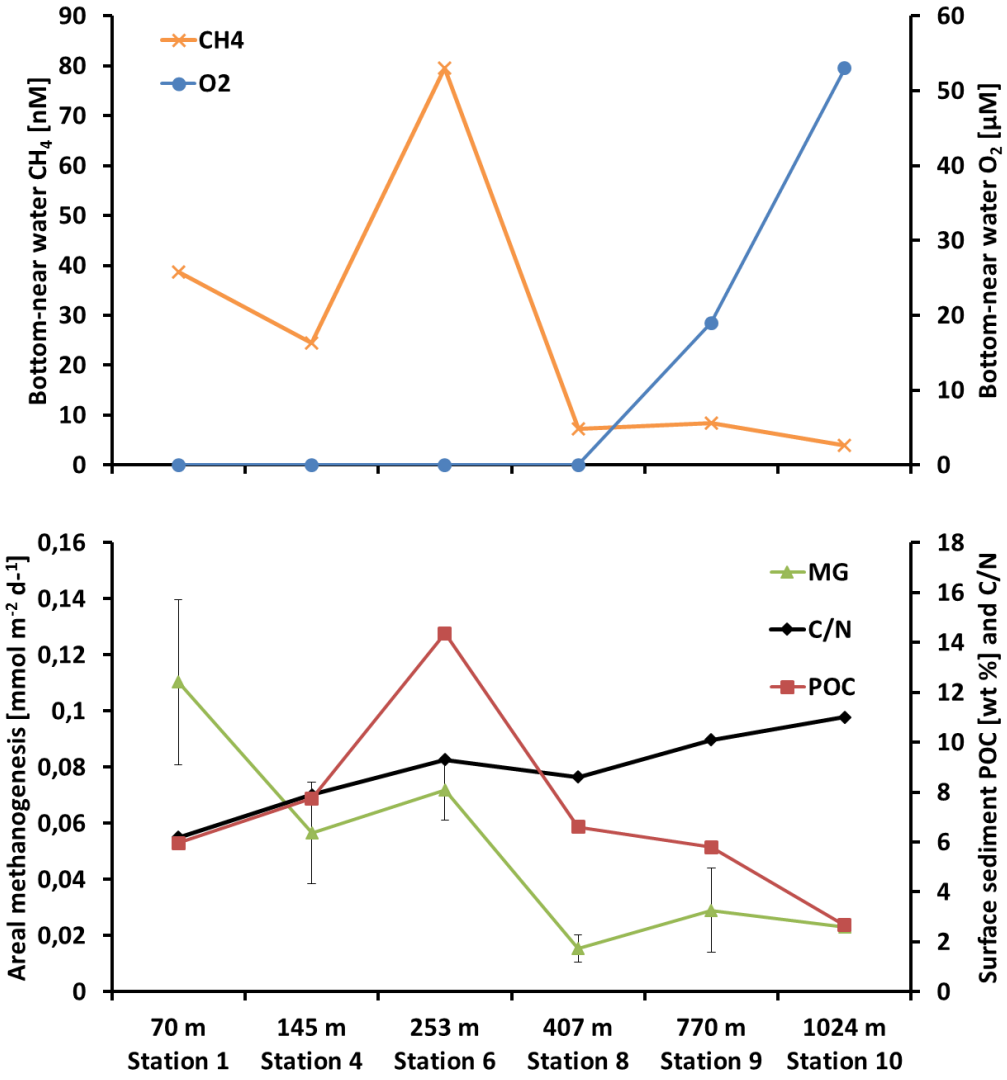
CH4
O2
Bottom-near water CH4 [nM]
Bottom-near water O2 [µM]
MG
C/N
POC
Areal methanogenesis [mmol m-2 d-1]
Surface sediment POC [wt %] and C/N
70 m
Station 1
145 m
Station 4
253 m
Station 6
407 m
Station 8
770 m
Station 9
1024 m
Station 10